Nanoswitches

DOI: 10.1002/anie.201400804

Bidirectional Chemical Communication between Nanomechanical Switches**

*Susnata Pramanik, Soumen De, and Michael Schmittel**

Abstract: *The interplay of biological machines depends critically on the bidirectionality of chemical information exchange. The implementation of such a communication procedure for abiological systems is achieved using two nanoswitches that both operate as transmitters and receivers by transfering copper ions in oxidation states + I and + II. Even at micromolar concentrations, communication in both directions is remarkably fast, occurring at $t_{1/2}$ = 2–3 min. Metal ion translocation triggers a 20 Å relocation of the toggle at both nanoswitches, entailing major geometric and electronic changes.*

Endogeneous and exogeneous communication is essential for life. From bacteria to animals, intricate processes,[1] such as *chemotaxis*[2] (motion towards food) and cell division,[3] are guided by chemical signal transduction, often even through entangled signaling cascades. Signal transduction in biology has to be specific and sensitive. Thus, it is a tremendous challenge for the new field of systems chemistry to establish fast bidirectional communication[4] using appropriate driving energy[4c,d] between artificial molecular devices and switches.[5–7] An elegant example of molecular communication that involves a tandem switching being reminiscent of proton relay processes in biology has recently been reported by Aprahamian.[4d] In that particular case, the addition of a zinc(II) ion changed the configuration and switching state of a hydrazone-based switch, which additionally initiated toggling of a second switch through translocation of a proton. To reset the system to its initial state, the metal ion needed to be removed by cyanide. As a consequence, reversible communication was unilaterally actuated through chemical inputs at the same switch while the second switch assumed a passive and externally operated role.[4c,d]

Herein, we present a procedure for reversible communication between the two nanoswitches **1** and **2**. Both experience major nanomechanical reorganization at the sending and the receiving nanoswitch and both are able to act as transmitters in the switching. Bidirectional communication is realized by translocation of copper in two redox states and may be triggered externally by chemical or electrochemical oxidation/reduction (Scheme 1). In detail, upon oxidation of complex $[Cu(\mathbf{1})]^+$ (state $\mathbf{1}^{II}_{Cu}{}^+$), the resultant copper(II) ion migrates to nanoswitch **2**, where it detaches the azaterpyridine arm from the zinc porphyrin station to form complex $[Cu(\mathbf{2})]^{2+}$ (state $\mathbf{2}^{II}_{Cu}{}^{2+}$). At the same time, that is, after releasing the Cu^{2+}, the azabipyridine arm of **1** moves to the zinc porphyrin station, generating state $\mathbf{1}^{I}$. Thus, in the communication process, both switches undergo a circa 20 Å nanomechanical reorganization at their arms. Reduction of state $\mathbf{2}^{II}_{Cu}{}^{2+}$ in presence of $\mathbf{1}^{I}$ resets the system by reconstituting the original switching states ($\mathbf{1}^{II}_{Cu}{}^+$ and $\mathbf{2}^{I}$).

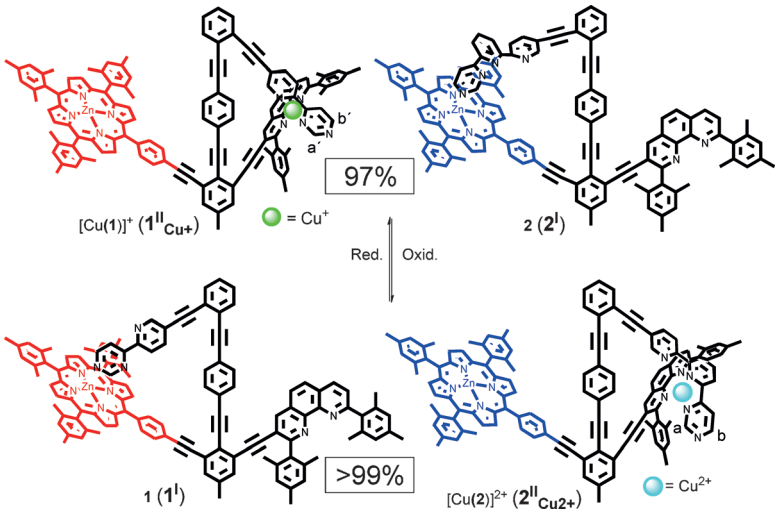

Scheme 1. Reversible bidirectional communication between two nanoswitches (the switching states are denoted in brackets).

We designed the reversible switching on the basis of three orthogonal coordination motifs, that include [Cu(phen1)(phen2)]$^+$ (HETPHEN), [Cu(phen)(terpy)]$^+$ (HETTAP), and pyridine→zinc porphyrin interactions[8] (phen = phenanthroline, terpy = terpyridine). In the recently reported nanoswitch **1**,[9] we combined HETPHEN and pyridine→zinc porphyrin interactions, while in the new nanoswitch **2** the latter interaction is opposed to a HETTAP complexation site. As demonstrated earlier, Cu^+ favors the HETPHEN coordination, while Cu^{2+} ought to prefer the pentacoordinated

[*] S. Pramanik, S. De, Prof. Dr. M. Schmittel
Center of Micro and Nanochemistry and Engineering
Organische Chemie I, Universität Siegen
Adolf-Reichwein-Strasse 2, 57068 Siegen (Germany)
E-mail: schmittel@chemie.uni-siegen.de

[**] We are grateful to the Deutsche Forschungsgemeinshaft and the Universität Siegen for financial support. We thank Debrata Samanta for PM6 calculations, Dr. T. Paululat for NMR measurements, and Kun Chen for the biferrocenyl derivative.

Supporting information for this article is available on the WWW under http://dx.doi.org/10.1002/anie.201400804.

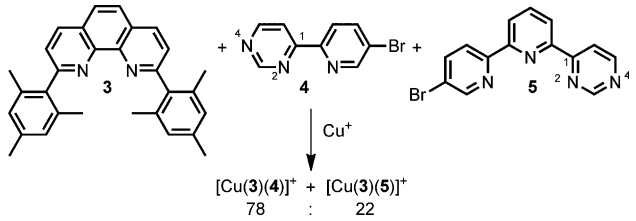

Scheme 2. Selectivities of model ligands towards Cu^+.

HETTAP situation, in analogy to procedures elaborated by Sauvage in redox-controlled molecular machinery.[10]

Before preparation of **2** made enough sense, we needed at first to evaluate orthogonal functioning of its prospective azaterpyridine arm face to face with the azabipyridine unit in **1.** Thus, in a model study (Scheme 2) a 1:1:1:1 mixture of **3**, **4**, **5**,[11] and Cu^+ was reacted in [D_2]dichloromethane, furnishing $[Cu(\mathbf{3})(\mathbf{4})]^+$ and $[Cu(\mathbf{3})(\mathbf{5})]^+$ in a ratio of 78:22, as derived from ^{1}H NMR spectroscopy (Supporting Information, Figure S1). As a result, preferentially $[Cu(\mathbf{1})]^+$ (state $\mathbf{1}^{\mathbf{II}}{}_{Cu}{}^+$) should form from a 1:1:1 mix of Cu^+, **1**, and **2**. The relative ratio of $[Cu(\mathbf{1})]^+$ vs. $[Cu(\mathbf{2})]^+$, however, would even be enlarged if intramolecular binding in $\mathbf{2}^{\mathbf{I}}$ were stronger than that in $\mathbf{1}^{\mathbf{I}}$. To predict partitioning of Cu^+ to both switches, we undertook computations at the PM6 level. The minimized structure of switch $\mathbf{1}^{\mathbf{I}}$ shows the azabipyridine ^{4}*N*-terminus to be significantly off the ideal axial coordination to the zinc porphyrin, suggesting some amount of strain in the molecule (see Computational Studies in the Supporting Information). Conversely, switch $\mathbf{2}^{\mathbf{I}}$ may experience less strain[12] because the azaterpyridine ^{4}N-atom coordinates almost perpendicularly (at 87.4°) to the zinc porphyrin.

Synthesis and characterization of **1** and $[Cu(\mathbf{1})]^+$ have been reported recently.[9] Nanoswitch **2** was prepared in 30% yield by Sonogashira coupling from its direct precursors (Supporting Information, Scheme S1) and was fully characterized using ^{1}H NMR, IR, and UV/Vis spectroscopy, ESI-MS, and elemental analysis. The ESI mass spectrum displays a molecular ion peak at $m/z = 1813.7$ that is diagnostic for $[\mathbf{2}{\cdot}H]^+$ with the observed isotopic distribution neatly matching the theoretical one (Supporting Information, Figure S3). In the ^{1}H NMR, the pyrimidine protons a-H and b-H show up in the aliphatic region at 3.57 and 2.72 ppm (Figure 1a; Supporting Information, Figure S2), respectively, clearly suggesting coordination of the ^{4}N nitrogen to the zinc porphyrin and thus state $\mathbf{2}^{\mathbf{I}}$ (Scheme 3). Furthermore, the UV/Vis absorption band at 429 nm (Soret band, $c_{(2)} = 10^{-6}$ M) corroborates the pyrimidine unit to be bound to the zinc porphyrin. Concentration independence of the wavelength and the extinction coefficient provides convincing evidence for intramolecular coordination (Supporting Information, Figure S4).

At first, we investigated toggling between the two states $\mathbf{2}^{\mathbf{I}} \rightarrow \mathbf{2}^{\mathbf{II}}{}_{Zn}{}^{2+}$ of the new nanoswitch using one equiv of Zn^{2+} as a diamagnetic input. The ^{1}H NMR for $[Zn(\mathbf{2})]^{2+} = \mathbf{2}^{\mathbf{II}}{}_{Zn}{}^{2+}$ (Figure 1c; Supporting Information, Figure S5) exhibits downfield shifts $\Delta\delta$ of 4.72 and 5.88 ppm for the pyrimidine protons a-H and b-H, respectively, suggesting the formation of a zinc(II) phenanthroline terpyridine complex. This assignment is further corroborated by diagnostic upfield shifts of the

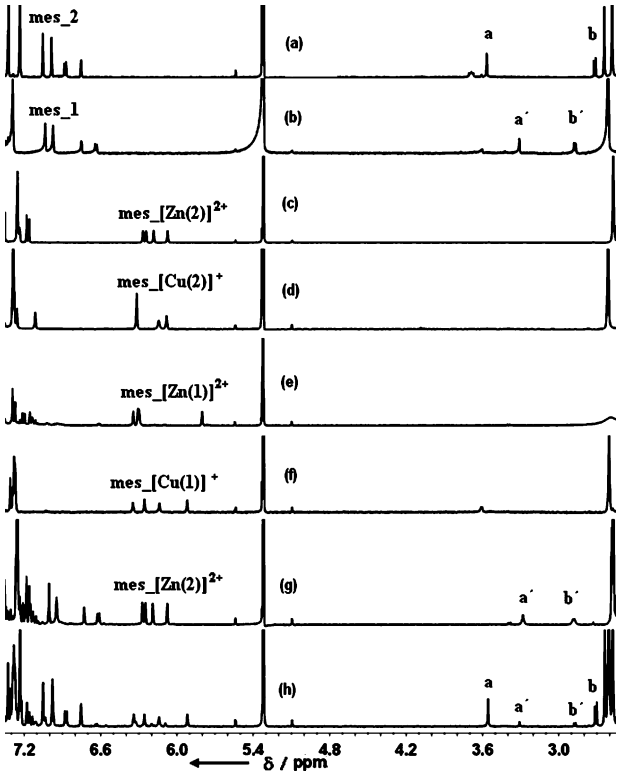

Figure 1. ^{1}H NMR (400 MHz, 298 K, CD_2Cl_2) of a) switch **2**; b) switch **1**; c) $[Zn(\mathbf{2})]^{2+}$; d) $[Cu(\mathbf{2})]^+$; e) $[Zn(\mathbf{1})]^{2+}$; f) $[Cu(\mathbf{1})]^+$; g) mixture of **1** and **2** in presence of Zn^{2+}; and h) mixture of **1** and **2** in presence of Cu^+.

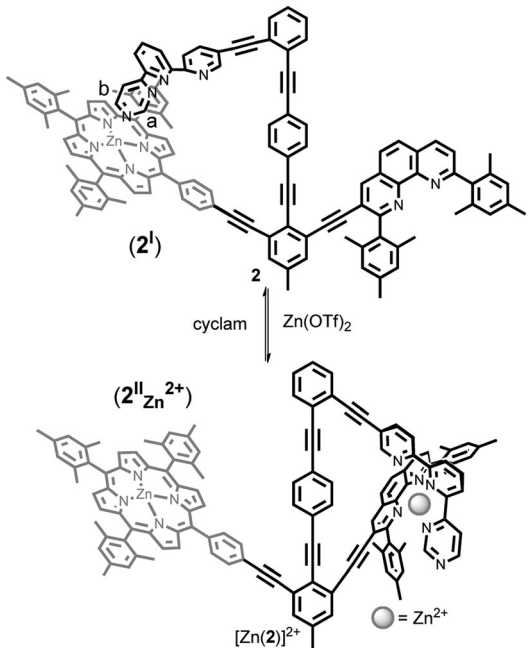

Scheme 3. Reversible toggling between two states of switch **2**. $Zn(OTf)_2$ has to be added in CD_3CN owing to solubility problems.

mesityl protons from 6.98 and 7.05 ppm to 6.07, 6.18, 6.24, and 6.27 ppm, as the protons are now shielded by the azaterpyridine unit. Splitting into four signals arises owing to constitutional and geometrical unsymmetry in the complex. Likewise,

the characteristic downfield shifts $\Delta\delta$ of phenanthroline protons 4-H and 7-H by 0.74 and 0.70 ppm, respectively, verify formation of $\mathbf{2^{II}}_{Zn}{}^{2+}$. A shift of the Q-band from 562 to 550 nm in the UV/Vis titration of **2** (10^{-4} M) with one equiv of Zn^{2+} (2.5×10^{-3} M) indicates a detachment of the azaterpyridine arm from the zinc porphyrin station (Supporting Information, Figure S13). The ESI mass spectrum shows a molecular ion peak at $m/z = 939.1$, the experimental isotopic distribution of which precisely matches the theoretical pattern for $[Zn(\mathbf{2})]^{2+}$ (Supporting Information, Figure S7).

Toggling was completely reversed to state $\mathbf{2^{I}}$ upon removal of zinc(II) ions from $\mathbf{2^{II}}_{Zn}{}^{2+}$ by complexation with one equiv of cyclam. Hereupon, the azaterpyridine arm reverts back to the zinc porphyrin station as proven by NMR and UV/Vis spectroscopy and in comparison with state $\mathbf{2^{I}}$. In the ^{1}H NMR spectrum ($c = 0.55$ mM), for example, protons a-H and b-H reappear at their initial positions (3.57 and 2.72 ppm) as do the mesityl protons at 6.98 and 7.05 ppm when 1 equiv of cyclam was added. Reversibility of the process was demonstrated over two and a half cycles by ^{1}H NMR spectroscopy (Supporting Information, Figure S12). For additional support, a UV/Vis titration of $[Zn(\mathbf{2})]^{2+} = \mathbf{2^{II}}_{Zn}{}^{2+}$ (10^{-4} M) against cyclam ($2.5\times10-3$ M) was conducted. The shift of the Q-band from 550 to 562 nm indicated formation of $\mathbf{2^{I}}$. However, owing to the lower concentrations in the UV/Vis titration, 1.5 equiv of cyclam was required (Supporting Information, Figure S14).

To evaluate the unidirectional communication, nanoswitches $[Zn(\mathbf{1})]^{2+}$ (Figure 1e) and $[Cu(\mathbf{2})]^{+}$ (Figure 1d) were prepared separately.[13] Upon mixing of $[Zn(\mathbf{1})]^{2+}$ and **2** in [D$_2$]dichloromethane, translocation of the zinc ion from $\mathbf{1^{II}}_{Zn}{}^{2+}$ to $\mathbf{2^{I}}$ thus generating states $\mathbf{1^{I}}$ and $\mathbf{2^{II}}_{Zn}{}^{2+}$ was monitored by ^{1}H NMR spectroscopy and ESI-MS. For solubility purposes, the mixture had to be heated first at 40 °C for a few seconds to dissolve compound **2**. A subsequently recorded ^{1}H NMR spectrum of the reaction mixture (Figure 1g) was devoid of the three sets of mesityl protons that are indicative for $[Zn(\mathbf{1})]^{2+}$ showing instead signals typical for **1**, for example the two singlets at 6.97 and 7.03 ppm. Indicative of **1**, pyrimidine protons a′-H and b′-H now emerge at 3.31 and 2.88 ppm, respectively. The mesityl protons related to $[Zn(\mathbf{2})]^{2+} = \mathbf{2^{II}}_{Zn}{}^{2+}$ appear upfield at 6.07, 6.18, 6.24, and 6.27 ppm as four peaks. Protons a-H and b-H show up at 8.29 and 8.60 ppm, respectively (Supporting Information, Figure S15). ESI-MS data corroborate the full metal ion exchange, displaying only $[Zn(\mathbf{2})]^{2+}$ at $m/z = 939.1$ (Figure 2, bottom). As a result, a battery of data clearly shows quantitative translocation of Zn^{2+} between $[Zn(\mathbf{1})]^{2+}$ and **2** to afford $[Zn(\mathbf{2})]^{2+}$ and **1**, that is, a directional communication between nanoswitches in states $\mathbf{1^{II}}_{Zn}{}^{2+}$ and $\mathbf{2^{I}}$ generating the switches in the final states ($\mathbf{1^{I}}$ and $\mathbf{2^{II}}_{Zn}{}^{2+}$).

Reverse metal-ion translocation was studied by a similar procedure; however, now using copper(I) ions. Complex $[Cu(\mathbf{2})]^{+}$ was prepared separately in [D$_2$]dichloromethane, then **1** was added. The communication of nanoswitches $\mathbf{1^{I}}$ and $\mathbf{2^{II}}_{Cu}{}^{+}$ by copper(I) ion translocation led to the nanoswitches in states $\mathbf{1^{II}}_{Cu}{}^{+}$ and $\mathbf{2^{I}}$. While in CD_2Cl_2, the translocation stopped at 90% conversion, that is, the mixture contained 90% of $[Cu(\mathbf{1})]^{+} = \mathbf{1^{II}}_{Cu}{}^{+}$ and 10% of $[Cu(\mathbf{2})]^{+} = \mathbf{2^{II}}_{Cu}{}^{+}$ (see ^{1}H NMR spectra in Figure 1h and the Supporting Information, Figure S18), the selectivity was increased to 97:3 ($[Cu(\mathbf{1})]^{+}$/$[Cu(\mathbf{2})]^{+}$) by adding 2% (*v*/*v*) CD_3CN as a weakly coordinating solvent (Supporting Information, Figure S20).[12] In the translocation process, the three peaks related to mesityl protons of $[Cu(\mathbf{2})]^{+}$ at 6.08, 6.14, and 6.32 ppm decrease and a new set with four mesityl protons at 5.92, 6.14, 6.26, and 6.34 ppm emerges for $[Cu(\mathbf{1})]^{+}$. Additionally, a new set of peaks appears at 3.55 and 2.71 ppm, which is characteristic for free **2** with its azaterpyridine protons a-H and b-H being located in the shielding region of the zinc porphyrin ring. The translocation of Cu^{+} was equally seen in the ESI mass spectra. Upon changing from dichloromethane (Figure 2, top) to dichloromethane/2% acetonitrile (Supporting Information, Figure S22) the peak of complex $[Cu(\mathbf{1})]^{+}$ at $m/z = 1799.2$ is further enlarged.

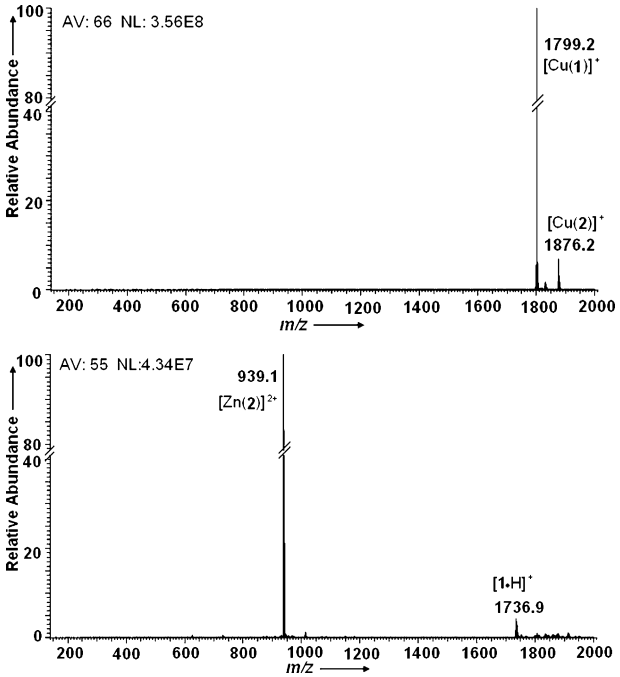

Figure 2. ESI mass spectra of (top) a mixture of **1**, **2** and Cu^{+} (1:1:1) suggesting a ratio of both complexes $[Cu(\mathbf{1})]^{+}/[Cu(\mathbf{2})]^{+} \approx 90{:}10$, as corroborated by NMR integration; (bottom) a mixture of **1**, **2**, and Zn^{2+} (1:1:1) showing exclusive formation of $[Zn(\mathbf{2})]^{2+}$, as substantiated by the NMR data (Figure 1g).

Initial kinetic measurements for metal ion translocation were conducted at 25 °C. At first, the kinetics of Zn^{2+} translocation from $[Zn(\mathbf{1})]^{2+}$ to **2** was evaluated (at $c =$ 2.56 mM) in $CDCl_3$. When the NMR spectrum was recorded 6 min after mixing, it indicated that 90% translocation had already taken place. The translocation was clearly completed 16 minutes after mixing (Supporting Information, Figure S16). A kinetic analysis at $c = 2.5\times10^{-6}$ M for each of $[Zn(\mathbf{1})]^{2+}$ and **2** showed a pseudo-first-order course, providing $t_{1/2} = 161$ s (25 °C; see "Translocation of metal ions" in the Supporting Information). Similarly, the Cu^{+} translocation was followed in the ^{1}H NMR after adding one equivalent of nanoswitch **1** to $[Cu(\mathbf{2})]^{+}$ (both at 2.78 mM). Six minutes after mixing, the system had already reached its final equilibrium

position (Supporting Information, Figure S19). A more accurate analysis by UV/Vis spectroscopy showed $t_{1/2} = 102$ s (25 °C) and pseudo-first-order behavior (both reactants used at $c = 5 \times 10^{-6}$ M). The two metal ion translocations are thus kinetically independent of the concentration of the metal-free nanoswitch, implying that the rate-limiting step involves an intramolecular dissociation of the metal complex = state II. Moreover, because the translocation of both Cu^{+} and Zn^{2+} ions proceeds within a few minutes, the communication is of rather similar speed in both directions.

After these promising results, we checked for bidirectional reversible redox-controlled copper ion translocation. A solution (1:1:1) of **1**, **2**, and $[Cu(CH_3CN)_4]B(C_6F_5)_4$ in dichloromethane ($c = 0.80$ mM), thus of $[Cu(\mathbf{1})]^{+}$ and **2**, served as the starting point.[15] A scan to anodic potential in a cyclic voltammetry (CV) experiment revealed a small oxidation wave at 0.25 V_{SCE} for $[Cu(\mathbf{2})]^{+/2+}$ (10%) and a large oxidation current at circa 0.75 V_{SCE} for $[Cu(\mathbf{1})]^{+/2+}$ (Supporting Information, Figure S33). Unfortunately, no Cu^{2+} translocation from $[Cu(\mathbf{1})]^{2+}$ to **2** generating $[Cu(\mathbf{2})]^{2+}$ was recognized on the CV time scale in the reverse sweep, even when we used low scan rates, such as 50 mV s^{-1}. Equally, the translocation did not show up when the CV was stopped at the anodic switching potential for 60 s before starting the reductive scan. Such finding is in agreement with the slow rate of Zn^{2+} translocation taking place only within minutes (see above), as most likely Cu^{2+} will behave similarly owing to analogous coordination preferences. On the other side, exclusive formation of $[Cu(\mathbf{2})]^{2+}$ was detected in ESI-MS investigations 10 minutes after adding switch **2** to $[Cu(\mathbf{1})]^{2+}$ (Supporting Information, Figure S27). Because of the low concentrations (0.80 mM) and inadequate time scale of CV experiments, metal ion transfer is thus not detectable after oxidation in a single CV scan.

To probe the redox-initiated toggling on a slower time scale, we decided to use chemical redox agents. For oxidation, we chose tris(4-bromophenyl)aminium hexachloroantimonate ($TBPA^{\bullet+}SbCl_6^{-}$)[16] and for reduction, decamethylferrocene (dmfc)[17] or a 3-alkyl-1,1′-biferrocenylene (BFD).[18,19] To a mixture of $[Cu(\mathbf{1})]^{+}$ and **2** in dichloromethane (prepared as above), one equivalent of $TBPA^{\bullet+}$ was added. After 3 min, a reductive scan CV analysis that was started at $+1.0$ V_{SCE} (Supporting Information, Figure S34) showed a sharp increase in current at 0.25 V_{SCE}, suggesting increased formation of $[Cu(\mathbf{2})]^{2+}$. In ESI-MS, the molecular ion peak at $m/z =$ 939.1, assigned to the dicharged $[Cu(\mathbf{2})]^{2+}$, shows up almost exclusively (Figure 3, top). The resultant solution of $[Cu(\mathbf{2})]^{2+}$ was now reduced by adding 1 equiv of dmfc (Supporting Information, Figure S35). An oxidative scan started at -0.9 V_{SCE} 2 minutes after mixing exhibited a lower current signal for $[Cu(\mathbf{2})]^{+}$ and a larger signal for $[Cu(\mathbf{1})]^{+}$ (includes $Cu^{+/2+}$ and $por^{0/+\bullet}$ redox transitions) than in the initial state. Thus, reduction of $[Cu(\mathbf{2})]^{2+}$ with dmfc led to translocation of Cu^{+} ions to **1**. An ESI mass spectrum recorded 10 minutes after mixing displayed peaks at $m/z = 1799.2$ (major) and 1876.2 (minor) (Figure 3, bottom), indicative of $[Cu(\mathbf{1})]^{+}$ and $[Cu(\mathbf{2})]^{+}$, respectively, thus confirming return to the starting state. For quantification, backward translocation was monitored by ^{1}H NMR using BFD as reducing agent because its

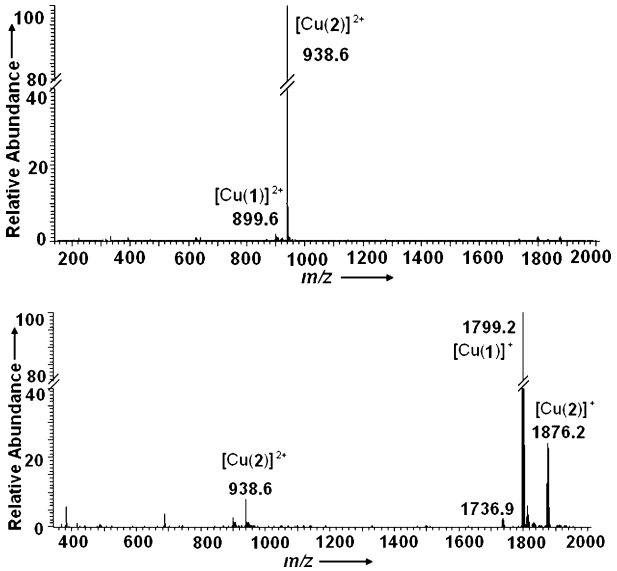

Figure 3. ESI-MS signature (top) of a solution containing **1**, **2**, and Cu^{+} (1:1:1) as obtained after oxidation with one equiv of $TBPA^{+\bullet}$ in CH_2Cl_2; (bottom) after reduction of the above solution with one equiv of dmfc.[14]

two-electron oxidation produces a diamagnetic species. In CD_2Cl_2, a $[Cu(\mathbf{1})]^{+}/[Cu(\mathbf{2})]^{+}$ ratio of 88:12 was observed, while in presence of 2% CD_3CN the ratio was improved to 95:5 (Supporting Information, Figure S30).[20]

Unfortunately, all attempts to monitor the kinetics of Cu^{2+} translocation by UV/Vis spectroscopy were met with failure owing to the fact that the absorbance changes are too small, but the rate of the process should to be similar to that of the Zn^{2+} translocation (see above).

In conclusion, we report herein on several examples of highly selective communication between two nanomechanical switches and their kinetics, as effected by intermolecular metal ion translocation. Even at micromolar concentrations, communication in both directions is fast occurring at $t_{1/2} = 2$–3 min with monomolecular metal-ion–ligand dissociation being the rate determining step. The metal ion translocation results in a circa 20 Å relocation of the toggle at both nanoswitches and thus to major geometric and electronic changes, similar as those in biological systems, that may allow to even link communication with switching ON/OFF (organo)catalysis.[21]

A reversible bidirectional communication is possible using chemical or electrochemical oxidation/reduction. Accordingly, oxidation of $[Cu(\mathbf{1})]^{+}$ and **2** with $TBPA^{+\bullet}$ leads to Cu^{2+} translocation furnishing **1** and $[Cu(\mathbf{2})]^{2+}$, while after reduction with dmfc or BFD the translocation of Cu^{+} yields the starting state = ($[Cu(\mathbf{1})]^{+}$ and **2**).

In summary, our work opens new vistas for systems chemistry, such as how to interconnect molecular computer and storage units or artificial synapses by chemical exchange processes. Such intermolecular switching is distantly reminiscent of that found in neural networks, relying on electrochemical signals between regions of the brain and spinal cord. Furthermore, communication between nanoswitches may be coupled to chemical follow-up processes.

Received: January 24, 2014
Published online: March 25, 2014

Keywords: chemical communication · nanoswitches · orthogonal coordination · redox reactions · reversible switching

[1] D. L. Nelson, M. M. Cox, *Lehninger Principles of Biochemistry, 4th ed.*, W. H. Freeman, New York, **2004**.

[2] a) R. M. Macnab, D. E. Koshland, Jr., *Proc. Natl. Acad. Sci. USA* **1972**, *69*, 2509; b) D. E. Koshland, Jr., *Science* **1977**, *196*, 1055.

[3] J. A. Knoblich, *Nat. Rev. Mol. Cell Biol.* **2001**, *2*, 11.

[4] a) F. M. Raymo, S. Giordani, *Org. Lett.* **2001**, *3*, 3475; b) S. Silvi, A. Arduini, A. Pochini, A. Secchi, M. Tomasulo, F. M. Raymo, M. Baroncini, A. Credi, *J. Am. Chem. Soc.* **2007**, *129*, 13378; c) S. C. Burdette, *Nat. Chem.* **2012**, *4*, 695; d) D. Ray, J. T. Foy, R. P. Hughes, I. Aprahamian, *Nat. Chem.* **2012**, *4*, 757.

[5] For some reviews, see: a) V. Balzani, A. Credi, S. Silvi, M. Venturi, *Chem. Soc. Rev.* **2006**, *35*, 1135; b) E. R. Kay, D. A. Leigh, F. Zerbetto, *Angew. Chem.* **2007**, *119*, 72; *Angew. Chem. Int. Ed.* **2007**, *46*, 72; c) S. Saha, J. F. Stoddart, *Chem. Soc. Rev.* **2007**, *36*, 77; d) B. Champin, P. Mobian, J.-P. Sauvage, *Chem. Soc. Rev.* **2007**, *36*, 358; e) V. Balzani, A. Credi, M. Venturi, *ChemPhysChem* **2008**, *9*, 202; f) K. Kinbara, T. Muraoka, T. Aida, *Org. Biomol. Chem.* **2008**, *6*, 1871; g) V. Balzani, A. Credi, M. Venturi, *Chem. Soc. Rev.* **2009**, *38*, 1542; h) P. Ceroni, A. Credi, M. Venturi, V. Balzani, *Photochem. Photobiol. Sci.* **2010**, *9*, 1561; i) S. Silvi, M. Venturi, A. Credi, *Chem. Commun.* **2011**, *47*, 2483; j) M. von Delius, D. A. Leigh, *Chem. Soc. Rev.* **2011**, *40*, 3656; k) J. E. Beves, B. A. Blight, C. J. Campbell, D. A. Leigh, R. T. McBurney, *Angew. Chem.* **2011**, *123*, 9428; *Angew. Chem. Int. Ed.* **2011**, *50*, 9260; l) A. Coskun, M. Banaszak, R. D. Astumian, J. F. Stoddart, B. A. Grzybowski, *Chem. Soc. Rev.* **2012**, *41*, 19.

[6] For some recent publications, see: a) N. Ruangsupapichat, M. M. Pollard, S. R. Harutyunyan, B. L. Feringa, *Nat. Chem.* **2011**, *3*, 53; b) T. Kudernac, N. Ruangsupapichat, M. Parschau, B. Maciá, N. Katsonis, S. R. Harutyunyan, K.-H. Ernst, B. L. Feringa, *Nature* **2011**, *479*, 208; c) M. J. Barrell, A. G. Campaña, M. von Delius, E. M. Geertsema, D. A. Leigh, *Angew. Chem.* **2011**, *123*, 299; *Angew. Chem. Int. Ed.* **2011**, *50*, 285; d) P. Lussis, T. Svaldo-Lanero, A. Bertocco, C.-A. Fustin, D. A. Leigh, A.-S. Duwez, *Nat. Nanotechnol.* **2011**, *6*, 553; e) G. T. Carroll, G. London, T. F. Landaluce, P. Rudolf, B. L. Feringa, *ACS Nano* **2011**, *5*, 622; f) G. Haberhauer, *Angew. Chem.* **2011**, *123*, 6539; *Angew. Chem. Int. Ed.* **2011**, *50*, 6415; g) H. Li, A. C. Fahrenbach, A. Coskun, Z. Zhu, G. Barin, Y.-L. Zhao, Y. Y. Botros, J.-P. Sauvage, J. F. Stoddart, *Angew. Chem.* **2011**, *123*, 6914; *Angew. Chem. Int. Ed.* **2011**, *50*, 6782; h) A. S. Lubbe, N. Ruangsupapichat, G. Caroli, B. L. Feringa, *J. Org. Chem.* **2011**, *76*, 8599.

[7] a) J. Ma, Y. Li, T. White, A. Urbas, Q. Li, *Chem. Commun.* **2010**, *46*, 3463; b) X. Su, T. F. Robbins, I. Aprahamian, *Angew. Chem.* **2011**, *123*, 1881; *Angew. Chem. Int. Ed.* **2011**, *50*, 1841; c) Y. S. Chong, B. E. Dial, W. G. Burns, K. D. Shimizu, *Chem. Commun.* **2012**, *48*, 1296; d) J. V. Gavette, N. S. Mills, L. N. Zakharov, C. A. Johnson II, D. W. Johnson, M. M. Haley, *Angew. Chem.* **2013**, *125*, 10460; *Angew. Chem. Int. Ed.* **2013**, *52*, 10270.

[8] a) M. Schmittel, K. Mahata, *Inorg. Chem.* **2009**, *48*, 822; b) K. Mahata, M. Schmittel, *J. Am. Chem. Soc.* **2009**, *131*, 16544; c) K. Mahata, M. L. Saha, M. Schmittel, *J. Am. Chem. Soc.* **2010**, *132*, 15933; d) M. L. Saha, S. De, S. Pramanik, M. Schmittel, *Chem. Soc. Rev.* **2013**, *42*, 6860.

[9] M. Schmittel, S. Pramanik, S. De, *Chem. Commun.* **2012**, *48*, 11730.

[10] a) J.-P. Sauvage, *Acc. Chem. Res.* **1998**, *31*, 611; b) J.-P. Collin, C. Dietrich-Buchecker, P. Gaviña, M. C. Jiminez-Molero, J.-P. Sauvage, *Acc. Chem. Res.* **2001**, *34*, 477.

[11] S. De, S. Pramanik, M. Schmittel, *Dalton Trans.* **2013**, *42*, 15391.

[12] The larger intramolecular strain in switch **1** can be easily verified. In presence of CD_3CN, a weakly coordinating solvent, the arm will become more detached from the porphyrin station the more strained the system is. As anticipated, the ratio of $[Cu(\mathbf{1})]^+$ versus $[Cu(\mathbf{2})]^+$ is increased from 90:10 to 97:3 with 2% CD_3CN (*v*/*v*) added (Supporting Information, Figure S20).

[13] For a detailed assignment, see the Supporting Information, Figures S8–S11.

[14] Masses are depicted above $m/z = 350$ to exclude the intense peak of $dmfc^+$ in the mass spectrum.

[15] CV spectra of the compounds $[Cu(\mathbf{1})]^+$ and $[Cu(\mathbf{2})]^+$ are shown in the Supporting Information, Figures S31 and S32, respectively.

[16] F. A. Bell, A. Ledwith, D. C. Sherrington, *J. Chem. Soc. C* **1969**, 2719.

[17] N. G. Connelly, W. E. Geiger, *Chem. Rev.* **1996**, *96*, 877.

[18] a) R. Breuer, M. Schmittel, *Organometallics* **2012**, *31*, 6642; b) R. Breuer, M. Schmittel, *Organometallics* **2013**, *32*, 5980.

[19] Oxidation potentials: $E_{1/2}\,(dmfc)^{[17]} = -0.160\ V_{SCE}$; $E_{1/2}\,(BFD) = 0.09\ V_{SCE}$ and $E_{1/2}\,(BFD^{+\bullet})^{[18]} = 0.76\ V_{SCE}$; reduction potential: $E_{1/2}\,(TBPA^{+\bullet}) = 1.06\ V_{SCE}$ (W. Schmidt, E. Steckhan, *Chem. Ber.* **1980**, *113*, 577).

[20] To monitor the reverse metal ion translocation by NMR spectroscopy, we started from a solution of $[Cu(\mathbf{2})]^{2+}$ and **1** (one equiv each) and added 3-(11-bromoundecyl)-1,1′-biferrocenylene as reductant (Supporting Information, Figure S30).

[21] M. Schmittel, S. De, S. Pramanik, *Angew. Chem.* **2012**, *124*, 3898; *Angew. Chem. Int. Ed.* **2012**, *51*, 3832.

